Effect of milling process on particle size, morphology and magnetization in non-stoichiometric Fe_2O_3-MnO_2.

P.Vera-Serna[1], M.A. Martínez-Sánchez[1], Martin Kusy[2], A.M.Bolarín-Miró[3], F.N.Tenorio-González[1], J.A.Juanico-Loran[4].

[1] División de Ingeniería, Universidad Politécnica de Tecámac, Tecámac 55740,
Phone: +525559388670, Mexico.
pedrovera.upt@gmail.com
[2] Faculty of Materials Science and Technology,
Slovak University of Technology in Bratislava, Trnava, Slovak Republic
[3] Área Académica de Ciencia de la Tierra y Materiales,
Universidad Autónoma del Estado de Hidalgo, Mineral de la Reforma, Mexico
[4] División de Ingeniería Industrial Nanotecnología,
Polytechnic University of the Valley of Mexico, Tultitlan, Mexico

ABSTRACT

A ratio non-stoichiometric between Iron oxide III and excess of Manganese oxide III were milled during 12 hours in a high energy ball milling using four iron spheres of diameter 12.7 mm and two iron spheres of diameter 9.5 mm. The characterization by X Ray Diffractions showed the phases of precursor powder in all samples, this result indicated that the powder only was milled and the process did not produce reaction. Rietvel refinement of X Ray Diffraction Patterns showed variations on crystalline planes and deformations occasioned by milling process, while Scanning Electron Microscopy and Particle Size Analysis showed that the particle size decreased with the process, a result in this study was the variation on magnetization without chemical reaction under non-stoichiometric conditions and the agglomeration sizes observed on samples. For the products have the same morphology by process.

Keywords: Advanced process; materials; manganese; milling; crystallite; mechanochemical

INTRODUCTION

The processes used on the products and materials result from the characteristics or properties defined by customers or users[1, 2], in the advanced materials the process is a specific requirement to have a control on morphology, size particle, properties, structure, mechanical resistance, magnetization, electric resistance [3,4,5], on results published in different investigations on synthesis methods as co-precipitation, sol gel, ceramic, electrochemical, polyol, flame and others has been analyzed the characteristics and properties [4,6-11], in the case of high energy milling environmentally contributed in synthesis to avoid hazardous waste, it is a sustainable processes [12] and a simple method suitable for the production of powders composed of fine particles. There are two ways to carry out the synthesis, dry and

wet; the dry way is preferable because the reactions are faster and with a lower pollution level than the wet on [13]. To obtain good results in high energy milling technic, it is important to consider some parameters, as previously reported by Serkan Biyik et. al. [14], such as type and amount of process control agent, milling speed and duration, ball-to-powder weight ratio, size of the grinding medium, material of the vial and grinding balls, and extent of vial filling.

The interesting aspect to research about on properties on this material is the wide field of application they have, such as coatings, elements for microwave devices, polymer, sensors, medical devices, and optics [7, 8, 9]. Various works developed on the last decade using high energy milling showed results on material in ratio with magnetization, morphology, particle size, electric conductivity, synthesis, deformation, some materials used in the process were iron oxides, manganese oxides, it is because it could be cheaper than materials as the samario (Sm) and neodymium (Nd) [9,15,16]. The high-energy milling method presents a significant advantage over the heat treatment method because the temperatures used are at room temperature, and in some occasions only with the milling (without change of structure) [7], magnetic saturation increase and it is possible to have nanometer size in some particles, the studies in materials show evidence on results to materials with deformation in lattice array, cases in which there is no chemical reaction but the magnetization increase [17].

The objective of this paper is to describe the effect of dry high energy milling process of non-stoichiometric mixtures between MnO_2 and Fe_2O_3 after 12 h and demonstrate that magnetic properties can be changed using milling, a specific variable was the quantity of manganese oxide III however, some articles that include non-stoichiometric proportions, reported superior magnetic properties [17]. Additionally, this paper includes the explanation of crystallographic parameters, particle size and morphology in order to describe the observed magnetic properties.

METHODS AND MATERIALS

High energy milling

The dry milling procedures were performed in a Spex mill 8000D for 12 hours; iron oxide III (Sigma-Aldrich) and manganese oxide IV (Sigma-Aldrich) were used in stoichiometric ratio following the previous report [18], the proportions of MnO_2 in the various compositions are presented in Table 1. M0 was the reference composition wherein the precursor oxides were added in stoichiometric ratio mol:mol 1:1 to obtain a possible chemical reaction, whereas the other compositions contained excess MnO_2 and it were evaluated to know the effect of milling on different manganese oxide IV quantity. The milling was performed at room temperature, 4 balls of hardened steel with a diameter of 12.7 mm and two balls with a diameter of 9.5 mm were placed in a stainless steel vial in order to improve the mobility of spheres into vial [19, 20, 21].

Table 1. Ratios of excess of MnO2 with chemical stoichiometry and non-stoichiometry

Composition	MnO$_2$ ratio add on chemical stoichiometry	Chemical composition
M0	0%	Stoichiometry
M10	10%	Non-stoichiometry
M20	20%	Non-stoichiometry
M30	30%	Non-stoichiometry
M40	40%	Non-stoichiometry
M50	50%	Non-stoichiometry

Characterization

For structural characterization, a Philips PW1710 X-ray diffractometer with CoKα (1. 5812 Å) radiation was used. Patterns were collected in the 20-80° range in 0.05° increments (2θ). The Rietveld refinement was conducted using Maud software, and the results were then compared with those in the Inorganic Crystal Structure Database (ICSD). The magnetic saturation was evaluated using a micro vibrating sampler magnetometer (Micro Sense EV7, VSM-EV7). The morphology was determined by SEM (JEOL) at 15 kV.

RESULTS AND DISCUSSION

Figure 1 shows the hysteresis loop of samples obtained by milling process. The expected results are the increase in magnetization as manganese oxide III increase according on Eq. 1 reported by Bean, C. [22]:

$$I(H) = \sum_{n=1}^{N} I_n(H) f_n \bigg/ \sum_{n=1}^{N} f_n \tag{1}$$

Where I(H) is the magnetization of a mixture in a field of N types of particles, f_n is the volume fraction of the nth constituent and $In(H)$ is the magnetization of this constituent in a field H. The saturation magnetization of Fe$_2$O$_3$ is 0.25 emu/g [23] and the saturation magnetization of MnO$_2$ is 3 emu/g [24] so that and following the previews equation, the saturation magnetization in sample M0 with ratio 1:1 mol:mol is ˜1 emu/g and according the volume fraction, the saturation magnetization of other samples should increase when percentage of manganese oxide III increase.

Figure 1 revealed that the saturation magnetization does not correspond to the mixtures theory because the proportion of added MnO$_2$ is no co-dependent of material magnetization. In magnetization, the ordering of samples from less to top is M0, M10, M50, M30, M20 and M40, the maximum magnetic response was on surplus 40%, while on 50% decrease. The increase was not attributed to a change in the structure but instead served as a reference to determine which variables could be adjusted to increase the magnetic saturation. This variation was related to the work of Xin Zhanga et al. [25], who observed similar

behaviour showing that the particle size was related to the magnetic saturation, the process and MnO_2 generated different properties.
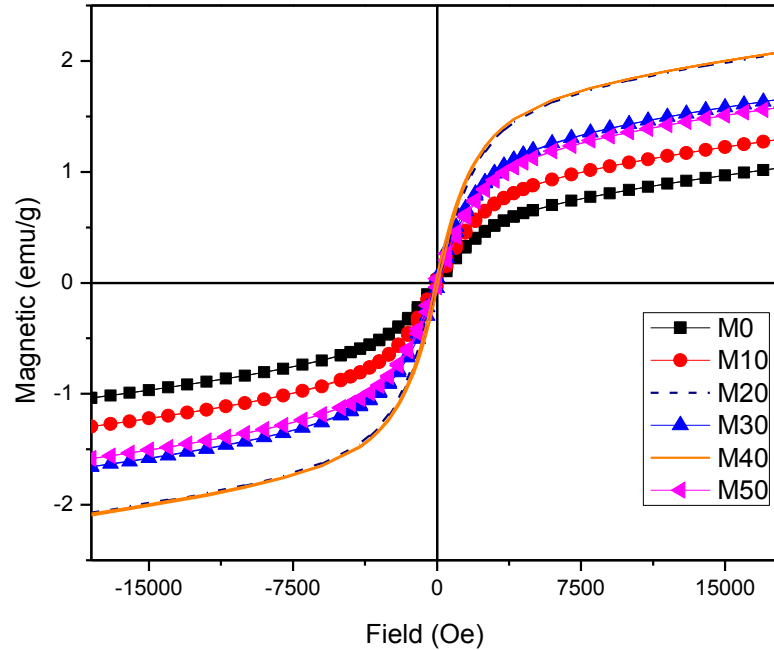
Figure 1. Hysteresis loops at Hmax=1800 Oe measured at room temperature of oxide powders milled from (MnO_2 + Fe_2O_3)

In order to confirm the previous statement, figure 2 shows the XRD results of M0, M20 and M40, they were selected to compare the stoichiometric with higher saturation magnetization samples. As it can be observed, three studies exhibited the same phases of MnO_2 and Fe_2O_3 for all samples tested with principal picks at 29° and 33° to manganese oxide III and iron oxide III subsequently.

An increase in the intensity of the signal at 29° and a decrement in the signal at 33 were observed witch shows that the picks at 33° in samples M0 and M20 is higher than picks at 29° however when the excess of manganese oxide III is 40%, picks change of intensity, in this powder the intensity of principal pick in MnO_2 is higher than Fe_2O_3. Intensity of principal picks confirm two things, on the one hand the increase in pick at 29° is due to greater percentage of MnO_2 in the powder and on the other hand, the percentage of phases ratifies the inconsistency in the magnetic properties following the mixtures theory.
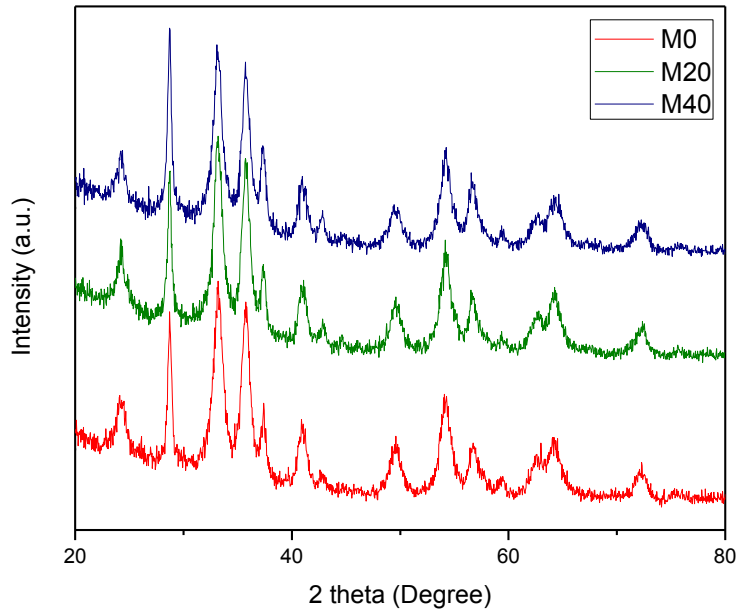
Figure 2. XRD of samples M0, M20 and M40 on 12 hours milling

In furtherance of intensity changes, in figure 3 a substratum of XRD from 25 to 35 degrees is presented showing the quantity values of intensity to samples M0 and M40. The intensity of pick at $29°$ in the sample M0 is 340 counts and increase at 425 counts when MnO_2 increase in 40% while the intensity of picks at $33°$ are about 420 counts in two samples because iron oxide III is constant.
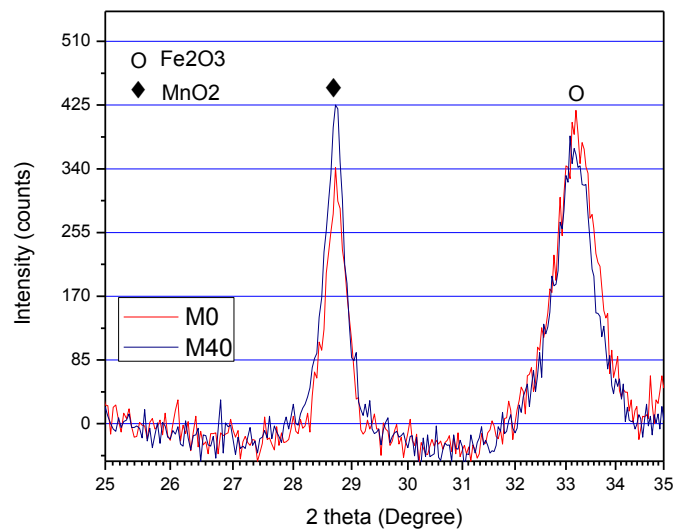
Figure 3. X-Ray profiles of M0 vs M40

Maud software was used for Rietveld refinement, the anisotropy of the material was identified and shown in Table 2. Different crystalline sizes can be identified on the planes of Fe_2O_3 and MnO_2, indicating the anisotropy of the material. This phenomenon may be attributable to the milling method employed, it causes deformations in crystal structure and Rietveld refinement method let crystallite sizes on milling M20 and M40 be observed, to identify differences.

The results show that because of the mechanical milling process, significant deformations exist on specific planes in MnO_2 to planes (1,1,0), (1,0,1) and (2,1,0) of M40, on M10 it was possible to detect an increase on plane (1,0,1), it could be the reason to have lower value of magnetic saturation in comparison with M40 and when M50 was evaluated, crystallite sizes grow.

Table 2. Crystallite sizes obtained by Rietveld refinement

Samples	Crystallite sizes							
	Phase	h, k, l 1, 0, 4	h, k, l 1, 1, 0	h, k, l 0,1,8	Phase	h, k, l 1, 1, 0	h, k, l 1, 0, 1	h, k, l 2,1,0
M0	Fe_2O_3	64	166	220	MnO_2	227	220	145
M10	Fe_2O_3	58	157	208	MnO_2	139	272	107
M20	Fe_2O_3	67	157	208	MnO_2	189	244	118
M30	Fe_2O_3	63	152	209	MnO_2	171	200	113
M40	Fe_2O_3	64	158	216	MnO_2	175	197	113
M50	Fe_2O_3	66	163	220	MnO_2	186	194	124

SEM images allowed the observation of the particles' irregular morphologies and their tendency to form agglomerates. The products have the same morphology, but especially among the images corresponding in Figure 4 (M10 and M50) had facility for making agglomerates bigger than other samples, while the smaller-sized particles in images on some circles in figure 4, this could be a possible relation between the magnetic response and sizes of agglomerates occasioned by the process when the particle is deformed and have different crystallite sizes.

The agglomerates with major diameter size absorb more energy and this condition could affect the response of the material when the magnetization is applied, this is possible when the results of Figure 1 are related and the crystallite sizes registered on Table 2, in this work it was possible to detect that with the increment of MnO_2 it is not necessary to have an increment of the value of magnetization in all the cases, with the results on SEM images, the results with milling on size particle on ratio in quantity of material added and values of magnetization it was possible know that the MnO_2 increment of the magnetization with certain sizes of agglomerates when the milling was used, the latter modifies the crystallite size on specific planes.
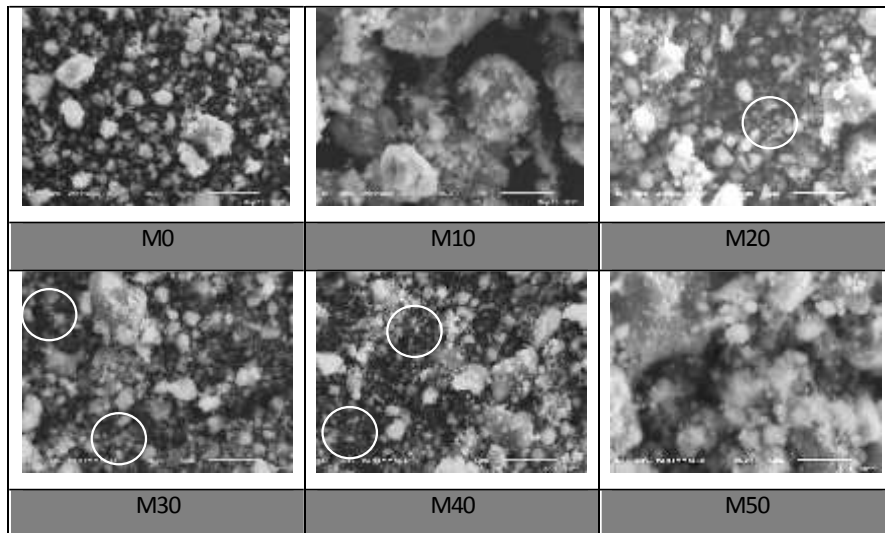
Figure 4. SEM images of M0, M10, M20, M30, M40 and M50 after 12 h of milling: particles with the lower size in circular line.

The particle sizes distribution was necessary to identify the variations caused by the milling process with a specific quantity of MnO_2, the analysis let us know the particle size detected in every case, so on the Figure 5 the particle size distribution was shown having smaller dimensions than M10 and M50 distribution on radius size the results are accord with images of SEM in Figure 5 and confirm the possibility to get the highest magnetic values on magnetization as wrote Dey et al. [26] and Singhal et al. [27] it is occasioned by the surface area, in this study only we only found a relation between with deformations and size particles, because in crystallography there were no changes on structure and when more quantity of MnO2 was added.
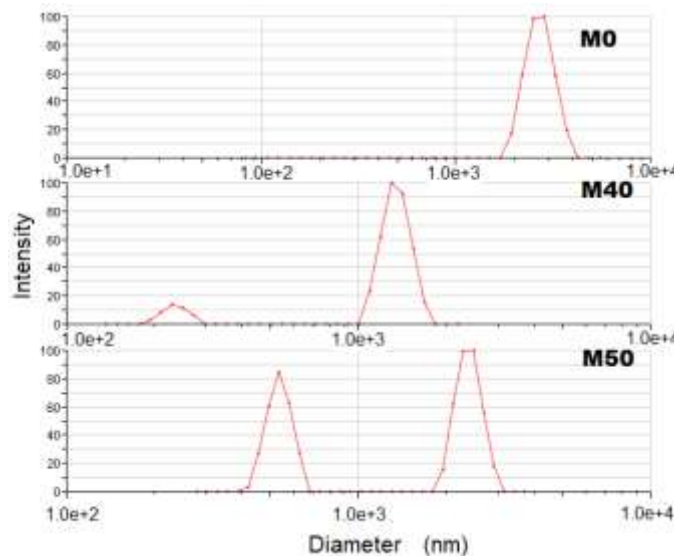
Figure 5. Particle Sizes Distribution on M0, M40 and M50 after 12 hours of milling

The Figure 6 shows the minimum size particle detected and it is possible to identify some the lowest dimension in milling of M40 in this study, while on M50 increase dimension, in the case of M10 there are a few particles with small size it also has agglomerate with higher dimension than M40 as was shown in Figure 5.
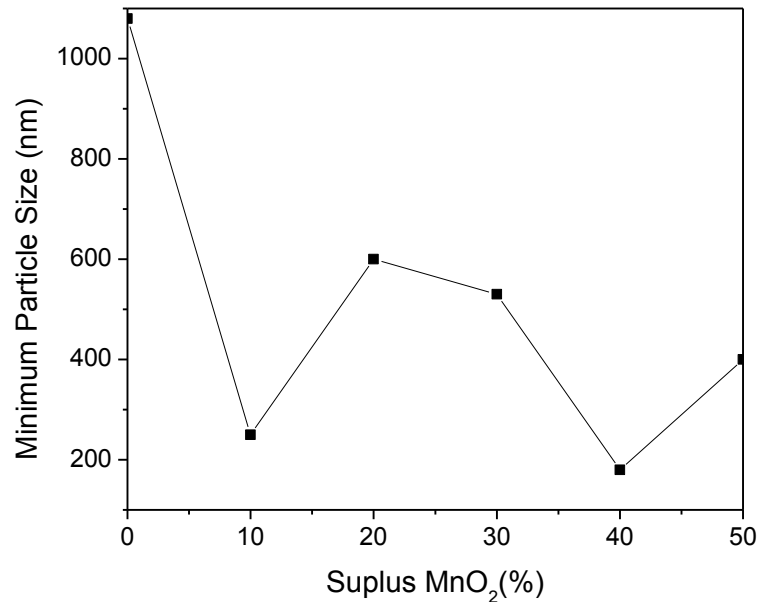
Figure 7. Particle Size Distribution vs MnO_2 added

CONCLUSIONS

The results by X Ray Diffraction demonstrated that the mechanical energy no-generate synthesis between start materials while the Rietveld refinement showed deformations in crystallite with smaller dimensions on specific planes of M20 and M40. The Samples increased the magnetization in material without direct dependence on MnO_2 quantity or spinel structure as studies were justified in various scientific articles published. On Scanning Electron Microscopy and Distribution Particle Size the samples M20 and M40 showed minor diameter in correspondence with other samples, the values of magnetization higher are on M20 and M40 hysteresis curves showed possible co-dependence between crystallite size, particle size and magnetization. A considerable factor was the possibility to develop materials without the need to have new phases or have necessary chemical stoichiometry, in an easier way, only with milling.

ACKNOWLEDGEMENTS

REFERENCES

[1] Lisha Geng1 L, and Lixiao Geng L. Analyzing and Dealing with the Distortions in Customer Requirements Transmission Process of QFD. Mathematical Problems in Engineering 2018; 2018 (4615320): 1–11

[2] Tekes E. Development of an expert system for demand management process. International Journal of Computer Integrated Manufacturing 2018; 31: 970-977

[3] Khan I, Saeed K, Khan I. Nanoparticles: Properties, applications and toxicities. Arabian Journal of Chemistry 2017;1-24. DOI: 10.1016/j.arabjc.2017.05.011

[4] Dung N.; Kyo-Seon K.; Controlled Magnetic Properties of Iron Oxide-Based Nanoparticles for Smart Therapy. Powder & Particle Journal 2016; 33: 33-47

[5] Laan D, Diem T, Hernandez M, Schiller H. Magnetic Chest Tube Positioning System. Journal of Medical Devices 2018; 12(2): 025001-025001-3

[6] Chen J, Gao X. Recent Advances in the Flame Synthesis of Carbon Nanotubes. American Journal of Materials Synthesis and Processing 2017; 2 (6): 71-89

[7] Achar TK, Bose A, Mal P. Mechanochemical synthesis of small organic molecules. Beilstein Journal Organic of Chemistry 2017; 13:1907–1931

[8] Lahiri I, Balasubramanian K. Application of mechano-chemical synthesis for protective coating on steel grinding media prior to ball milling of copper. Bulletin of Materials Science 2007; 30 (2): 157–161

[9] Mitsuru O, Hotta Y, Yamada M, Suzuki A, Futamoto M, Kirino F, Inaba, N. Structure of Sm-Co/Fe-Co multilayer films with in-plane magnetic anisotropies prepared on MgO(110) single-crystal substrates. Journal of Magnetism and Magnetic Materials 2016; 400: 253-261

[10] Donya R, Samira B, Sharifah BAH. Progress in electrochemical synthesis of magnetic iron oxide nanoparticles. Journal of Magnetism and Magnetic Materials 2014; 368: 207-229

[11] Chan TM, Levitin YY, Kryskiv OS, and Vedernikova IA, Characterization of Ag@Fe₃O₄core-shell nanocomposites for biomedical applications. Journal of Chemical and Pharmaceutical Research 2015; 7 (5): 816-819

[12] Cabras V, Aragoni MC, Coles SJ, Lai R, Pilloni M, Podda E, Ennas G. Mechanosynthesis of coordination polymers based on dithiophosphato and dithiophosphonato NiII complexes and 1, 4-di (3-pyridinyl) buta-1, 3-diyne ligand. Supramolecular Chemistry 2017; 29(11): 865-874.

[13] Tenorio FN, Barajas IR, Vera P, Sánchez F, Bolarin AM, Garrido A, Kusý M. Reducing the crystallite and particle size of SrFe12O19 with PVA by high energy ball milling. Journal of Alloys and Compounds 2019; 771: 464-470.

[14] Biyik, S, Arslan F, Aydin M. "Arc-Erosion Behavior of Boric Oxide-Reinforced Silver-Based Electrical Contact Materials Produced by Mechanical Alloying", Journal of Electronic Materials 2015; 44(1): 457-466.

[15] Ivo S, Katerina H, Kristyna P, Jan F, Mirka S.; Mechanochemical synthesis of magnetically responsive materials from non-magnetic precursors. Materials Letters 2014; 126: 202-206

[16] Zhong Y, Chaudhary V, Tan X, Parmarb H, Ramanujan RV. Mechanochemical synthesis of high coercivity Nd₂(Fe,Co)14B magnetic particles. Nanoscale 2017; 9: 18651-18660

[17]   Wanga GF, Zhaob ZR, Lib LR, Zhanga XF. Effect of non-stoichiometry on the structural, magnetic and magnetocaloric properties of $La_{0.67}Ca_{0.33}Mn_{1+\delta O3}$. Journal of Magnetism and Magnetic Materials 2016; 397: 198-204

[18]   Bolarín-Miró AM, Vera-Serna P., Sánchez-De Jesús F. Cortés-Escobedo CA, Martínez-Luevanos A. Mechanosynthesis and magnetic characterization of nanocrystalline manganese ferrites. Journal of Materials Science: Materials in Electronics 2011; 22 (8): 1046-1052.

[19]   Cai S, Tsuzuki T, Fisher TA, Nener BD, Dell JM, McCormick PG. Mechanochemical synthesis and characterization of GaN nanocrystals. Journal of Nanoparticle Research 2002; 4(4), 367-371.

[20]   Vera-Serna P, Bolarín-Miró A M, Sánchez-De Jesús F, Martínez-Luévanos A. Superficies y Vacío 2011; 24(2) 34-38.

[21]   Takacs L, McHenry JS. Temperature of the milling balls in shaker and planetary mills. J Mater Sci. 2006; 41:5246–5249. DOI 10.1007/s10853-006-0312-4

[22]   Bean CP. (1955). Hysteresis loops of mixtures of ferromagnetic micropowders. Journal of Applied Physics 1995; 26(11): 1381-1383.

[23]   Joshi DP, Pant G, Arora N, Nainwal S. Effect of solvents on morphology, magnetic and dielectric properties of (α-Fe_2O_3@SiO_2) core-shell nanoparticles. Heliyon 2017; 3(2): 1-16.

[24]   Zhou C, Wang J, Liu X, Chen F., Di Y, Gao S, Shi, Q. Magnetic and thermodynamic properties of α, β, γ and δ-MnO_2. New Journal of Chemistry 2018, 1:18

[25]   Xin Z, Yuping D, Hongtao G, Shunhua L, Bin W. Effect of doping MnO_2 on magnetic properties for M-type barium ferrite. Journal of Magnetism and Magnetic Materials 2007; 311 (2): 507-511

[26]   Dey S, Ghose J. Synthesis, characterisation and magnetic studies on nanocrystalline Co0. 2Zn0. 8Fe2O4. Materials Research Bulletin 2003; 38 (11-12): 1653-1660.

[27]   Singhal S, Namgyal T, Bansal S, Chandra K. Effect of Zn substitution on the magnetic properties of cobalt ferrite nano particles prepared via sol-gel route. Journal of Electromagnetic Analysis and Applications 2010; 2(06):376.